Al-Rafidain Journal of Engineering Sciences

Journal homepage https://rjes.iq/index.php/rjes

ISSN 3005-3153 (Online)

Using a Stand-Alone Wind Energy Conversion System as a Sustainable Technology to Produce Electricity in Iraq

[1,]Tamadhur Thamer Hashim, [2,*]Seref Kalem,

Electrical and Electronics Engineering Department, Bahçeşehir University, Istanbul, Turkey,

[1]tamaderal.2020@gmail.com [2]seref.kalem@bau.edu.tr

ARTICLE INFO

Article history:
Received 27 April 2024
Revised 10 May 2024,
Accepted 25 May 2024,
Available online 31 May 2024

Keywords:
vector control,
back-to-back converter frequency,
standalone wind generator

ABSTRACT

This work looks into Iraq's best places for wind turbines, with an emphasis on economic factors. It studies wind energy conversion systems using mathematical models from Matlab and Simulink. This research aims to pinpoint areas where wind energy can produce power on its own, separate from the national grid, for a range of applications, including energy storage, water pumps, heating, and cooling. In addition, the project will use PMSG to investigate wind turbine efficiency and create vector control technique technology for permanent magnet synchronous generators. Two Iraqi cities were taken to make the calculations of wind speed and its effect on electrical generations (Nasiriyah and Basra), where wind speeds of a height of 20 and 50 m were taken at the hub level of the turbine. The mechanical, electrical, and performance characteristics of the turbine were computed during the test to achieve optimal operation cases. The development of the system was done by MATLAB SIMULINK, where the overall efficiency was enhanced to 88.22%.

* Corresponding author E-mail address: seref.kalem@bau.edu.tr
https://doi.org/10.61268/mqayrh16

1. Introduction

The Iraqi Ministry of Electricity plans to integrate electric energy with renewable energy sources like wind, solar cells, and waste in the long term.

The ministry plans to collaborate with renewable energy companies like Siemens to implement $14 billion in projects, including a wind atlas and a 400 MW wind farm in Iraq, despite ongoing consideration from the Iraqi side [1]. The operation, control, and difficulties of converters are the main topics of this paper's review of their effects on the conversion of wind energy. It offers cutting-edge converter applications and suggestions for usage in the future with the goal of creating the best wind power technologies possible with increased cost, operation, and efficiency [2]. Wind energy needs to be carefully controlled and modeled for interconnection systems because it is utilized in big farms and off-grid systems. The advancement of wind turbine technology has resulted in their extensive usage [3]. Because wind turbine systems have a greater capacity and a greater impact on the electrical grid, converter technology has progressed greatly in wind power applications [4]. With the help of wind turbines and converter converters, the wind energy conversion system (WECS) transforms mechanical wind energy into electrical energy that is then transferred to a power network [5]. Because of improvements in semiconductor switch technology, generator rotor efficiency, dependability, and advanced materials, permanent magnet generators (PMG) are being used in wind turbines at an increasing rate [6]. Due to unfinished grid integration, WECS transforms wind kinetic energy into mechanical and electrical energy, requiring different converter topologies for grid-side and machine-side conversions [7]. Three configurations are used by wind turbines to convert wind energy into electricity: machine-terminal capacitors, utility power systems, and induction machines. These configurations all require reactive power to operate [8]. Wind energy can be converted into electricity using induction generators, and the most affordable and network-connected models are squirrel cage induction generators [9]. Wind energies, developed over 4000 years ago for mechanical energy in ships, mills, and agriculture, have been utilized in various regions and countries until the late 7th century for electricity production [10]. Wind turbines are categorized into horizontal and vertical axes, with horizontal axes being more efficient and common than vertical axes [11]. Iraq faces challenges in electric power demand due to infrastructure

development and an increasing local population, leading to a trend towards sustainable, environmentally friendly energy. Iraq's sustainable and renewable energy impact in 2018 was only 2% of electric energy use, with a goal to increase to 10% by 2030, but this is considered small [12]. Sustainable technologies like wind, solar, and tidal energy generate electric power without industrial waste, gases, or fumes, making them environmentally friendly and sustainable [13]. Wind energy, a rapidly growing and economically profitable sustainable technology, can be utilized to generate electric power in Iraq through self-financing and sustainable practices. In the paper [14], researchers developed a sustainable hybrid system for Iraqi electrical energy production using MATLAB, utilizing data from the Iraqi Meteorological Department. The study suggests Iraqi airspace could generate kicks from solar and wind energies while recommending independent systems for deserts and countryside [15]. A site study is crucial for maximizing wind energy utilization efficiency, considering factors like wind speeds, terrain, nearby forests, water, physiographic features, and study area characteristics [16–17]. To minimize the impact of forested areas, studies are conducted on forest and vegetation cover zones, tree growth, and wind potential. Wind measurements are taken throughout the year using a 35–40-meter wind measurement system. Wind turbines must ensure reliable and safe operation under specific wind conditions. Wind regimes are divided into normal and extreme conditions for safety and force effects on turbine components. The wind regime consists of constant averaged airflow and variable design wind gust profile or turbulence. The choice of wind speed distribution model significantly influences wind turbine design, as it determines the frequency of load changes on structural elements. The wind speed's height dependence in the surface layer is determined by wind speed measurements at different heights relative to the earth's surface.

Wind turbines operate in a turbulent environment, affecting the stability of their power system. Modeling shows that wind force spikes are converted into electrical power output, amplifying wind gusts. This is due to the nonlinearity of the energy conversion process and the rapid response of the output power to changes in wind speed. As wind speed decreases, the input power of the turbine decreases, reducing efficiency. Wind generator losses are divided into gearbox, inverter, and electric machine

losses. The relationship between wind speed and energy losses in the generator provides the entire picture of the turbine's efficiency. For wind speeds ranging from 5 to 14 m/s, the study shows how losses in the gearbox, SGPM, and AIN depend on the rotor speed of the PMSM rotor. The PMSM's losses increase with wind speed and are 71 W at 5 m/s. Losses in the gearbox vary from 25 to 71 W, while losses in the SGPM reach 647 W at 14 m/s. The study also reveals that as wind speed increases, losses in the gearbox and PMM increase, but their efficiency also increases. The study investigated the potential use of a displacement turbine in Iraq by computing its maximum mechanical power using a mathematical model [18]. The study examined the feasibility of wind turbine construction at 19 Iraqi stations and the potential of using wind dependency with Weibull distribution, presenting scientific findings and the wind's dynamic properties [19]. The study explores the use of wind turbines in Iraq for power generation, particularly for lighting parking lots, and their winter usage. The wind turbine model mathematically explains the conversion of mechanical energy into electrical energy, considering wind speed, efficiency, and turbine parameters for ideal output speed calculation [20, 21]. The research aims to create an independent wind energy system for irrigation, heating, and cooling poultry fields, combining three systems. It will use experimental work, real turbine models, wind speed data, and published studies. The study utilized data from the Iraqi Meteorological Authority and seismic monitoring from 2016–2017, focusing on Nasiriyah, Amarah, Basra Al-Hayy, and Al-Nasiriyah in southern Iraq [22]. Based on the study [23], daily wind speed values were obtained at a 3-meter tower height, used in 13 stations across 13 Iraqi governorates, using monthly wind speed levels. The article [24] studied the utilization of IoT in wind resource assessment as well as the life-time estimation of wind power modules. The model is created with many smaller sub-models of an aerodynamic rotor joined to a multi-pole generator as well as various sensors to retrieve wind data parameters. Simulations are carried out using Matlab/Simulink and Thingspeak, an IoT MathWorks web platform. IoT has so far demonstrated enhanced precision in measurements, monitoring, and quality control. The study [25] analyzed the graphical method (GM) and standard deviation method (SDM) applied to forecasting wind energy potential in Dar es Salaam, Tanzania. The wind speed data for 2017–2019 was obtained in the year 2020.

Both approaches were applicable for Weibull distribution parameter estimation. In this regard, SDM provided a better estimation value. We considered the Polaris P50-500 commercial wind turbine the best for our project since it had the highest capacity factor value (per annum) over the past 3 years.

Table 1 Sequences of Stations from North to South [25]

Stations Sequences from N to S	**Latitude (N)**	**Longitude (E)**	**Sea Level Altitude in Meters**
Mosul (Bashiqah)	36 45 09	43 33 88	228.0
Kirkuk (Daquq)	35 16 93	44 42 97	227.9
Salahaldeen (Tikrit)	34 65 28	43 63 61	116.0
Dealaa (Khalis)	33 75 17	44 62 22	40.9
Baghdad (Abughraib)	33 32 21	44 23 93	30.4
Anbar (Aldawar)	33 27 57	43 02 08	45.6
Wasat (Essaouira)	33 00 45	44 49 27	27.2
Karbla (Lake Razzaza)	32 33 20	43 58 37	49.0
Babel (Kifli)	32 30 63	44 39 16	21.1
Qadisiyah (Dewaneia)	32 01 93	44 89 85	24.0
Najaf (Mashkhab)	31 53 27	44 30 11	19.0
Mayssan (Ekhala)	31 48 04	47 11 25	9.0
The-Qar (Shatrah)	31 45 57	46 19 52	7.0
Muthna (Khader)	30 17 32	45 37 51	7.0
Basrah (Albrjsuh)	30 17 32	47 04 04	7.0

Wind speed increases with increasing altitude and distance from the terrain (2) [26-27].

$$\frac{\upsilon(z)}{\upsilon(z_0)} = \left(\frac{z}{z_0}\right)^{\frac{1}{7}}, \quad (1)$$

Z: height of wind speed.

v(z): wind speed.

v(z0): reference height and wind speed.

The wind speed is at three heights (12, 50, and 100 m).

2. Methodology

2.1 Mathematical Description of the Turbine Mode

The work W required to move an item from rest to a distance s under the influence of a force F is equal to the kinetic energy E of that object at constant acceleration a.

Newton's second law of motion states that [28]:

$$F = ma \tag{2}$$

So, the kinetic energy is equal to

$$E = mas \tag{3}$$

When it comes to solid motion kinematics $V^2 = U^2 + 2as$, where U is the initial speed of the object. This means that $a = \frac{v^2 - u^2}{2s}$ the initial speed of the object is zero, then Therefore, $a = \frac{v^2}{2s}$ from equation (3) we obtain the formula:

$$E = \frac{1}{2} m v^2 \tag{4}$$

The kinetic formulation of energy relies on the constant mass of a solid entity, while wind, treated like a liquid, may not have a constant mass due to potential fluctuations. The rate at which kinetic energy changes determines wind power P.

$$P = \frac{dE}{dt} = \frac{1}{2}\frac{dm}{dt} v_w^2 \tag{5}$$

The mass flow rate is determined by air density and A, representing the wind's passing region, resulting in Equation (6) being true.

$$P_w = \frac{1}{2}\rho A v_w^3 \tag{6}$$

The real mechanical power Pw, measured in watts and equal to the difference between input and output wind power, is extracted by the rotor blades.

$$P_w = \frac{1}{2}\rho A v_w (v_u^2 - v_d^2) \tag{7}$$

The downstream and upstream wind speeds at the rotor blade intake and outlet in meters per second are used to estimate the speed factor [20].

$$\rho A v_w = \frac{\rho A (v_u + v_d)}{2} \tag{8}$$

At the intake and outflow of the turbine's operating blades, the average air velocity is located. This expression produces equation (7).

Equation (7) is changed to equation (8) with the right side substituted, and the result is:

$$P_w = \frac{1}{2}\rho A v_w (v_u^2 - v_d^2)\frac{(v_u + v_d)}{2}$$

It is easier to understand as follows:

$$P_w = \frac{1}{2}\left[\rho A \left\{\frac{v_u}{2}(v_u^2 - v_d^2) + \frac{v_d}{2}(v_u^2 - v_d^2)\right\}\right]$$

$$P_w = \frac{1}{2}\left[\rho A \left\{\frac{v_u^3}{2} - \frac{v_u v_d^2}{2}) + \frac{v_d v_u^2}{2} - \frac{v_d^3}{2})\right\}\right]$$

$$P_w = \frac{1}{2}\left[\rho A v_u^2 \left\{\frac{1 - (\frac{v_d}{v_u})^2 + (\frac{v_d}{v_u}) - (\frac{v_d}{v_u})^3}{2}\right\}\right]$$

Or the following phrase might be used

$$P_w = \frac{1}{2}\rho A v_u^3 C_p \tag{9}$$

where C_p= $\left\{ \frac{1-(\frac{v_d}{v_u})^2+(\frac{v_d}{v_u})-(\frac{v_d}{v_u})^3}{2} \right\}$

Or

$$C_p = \frac{(1+\frac{v_d}{v_u})(1-\frac{v_d}{v_u})^2}{2} \quad (10)$$

The Betz limit, discovered in 1919, is the blade tip's upstream energy percentage, also known as rotor power factor or rotor efficiency. Its strength is determined by the wind turbine's rotational speed ratio [28].

$$\lambda = \frac{v_d}{v_u} \quad (11)$$

Or

$$\lambda = \frac{blade\ tip\ speed}{wind\ speed} \quad (12)$$

where (λ) is the speed (the speed of the turbine or the propeller's operating coefficient).

2.2 Users of the Wind Power Plant's Electrical Energy

Variations in current and voltage frequency result from wind turbines producing energy at wind speeds of two to three meters per second while running at lower power levels for longer periods of time. When operating on a linear active load, such as electric heaters, a wind turbine's power consumption (Pc) is exactly proportional to voltage (V squared).

$$P_c = P_{n1} \cdot (\frac{V}{V_n})^2, \quad (13)$$

P_c: power consumed by the electric heater.

P_{1n}: device power rated.

V: electrical appliance voltage falling.

V_n: electrical appliance rated voltage falling.

The maximum power P_{wt} developed by the wind turbine is proportional to the current frequency f to the cubic power:

$$P_{wt} = P_n \cdot (\frac{f}{f_n})^3, \quad (14)$$

P_{wt}: wind turbine power.

f: output frequency of wind generator.

P_{n2}: wind generator rated power.

f_n: the rated current frequency of the wind generator.

The generated power and consumed by a wind turbine can be determined by the connection between the generator's voltage and frequency, corresponding to ideal wind turbine-active load conditions.

$$\frac{V}{V_n} = (\frac{f}{f_n})^{3/2}, \quad (15)$$

An asynchronous motor may be driven by a standalone wind turbine, which requires an optimal voltage and frequency ratio [29]:

$$\frac{V}{V_n} = (\frac{f}{f_n}) \cdot (\frac{T_r}{T_n})^{1/2}, \quad (16)$$

T_r: current of load resistance moment.

T_n: nominal value of the moment of resistance of the load.

A converter is attached to rechargeable batteries, and after determining the generator's voltage and frequency, a brief description of the converter's requirements is formed.

2.3 *Types of PMSM-Based WECS*

PMSM motors are classified into radial and axial fields based on the flow of magnetic fields. Radial fields are commonly used due to their high flux density and energy acceleration, while axial fields have parallel field coherence. Surface-mount PMSMs, where permanent magnets are placed on the outer circumference of rotor plates, offer higher flux density but weaken the mechanical structure of the electrical machine, affecting its performance.

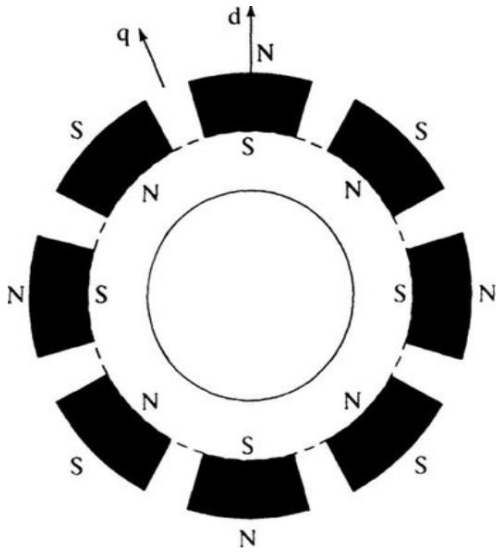

Figure 1. Surface permanent magnet [22].

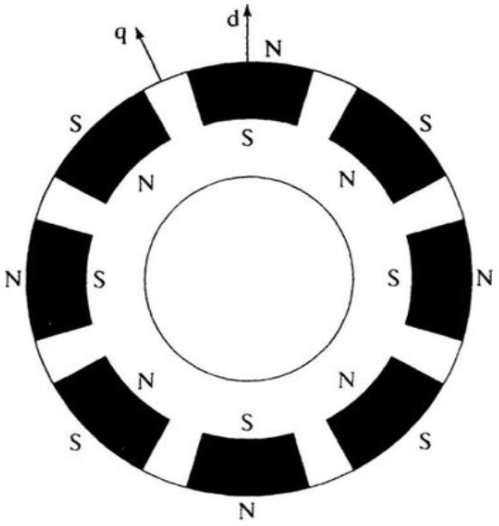

Figure 2. Surface insert a permanent magnet [30].

Other kinds involve laminating the magnet between plates inside the rotating portion of the electric motor, which depends on the placement of the magnet inside the spinning component.

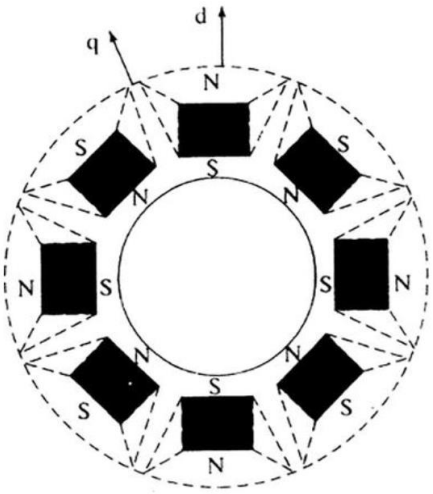

Figure 3. Interior permanent magnet [30].

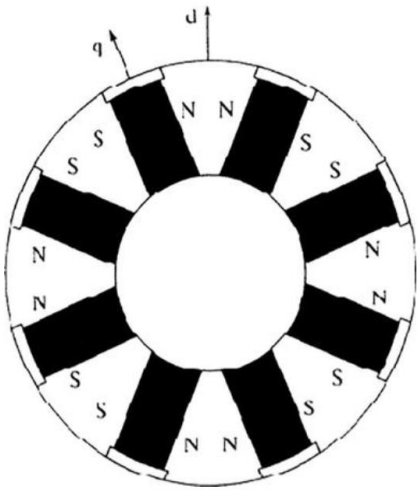

Figure 4. Interior permanent magnet with circumferential orientation [30].

PM machines are classified into two main parts: generator and engine, with various types listed in a chart.

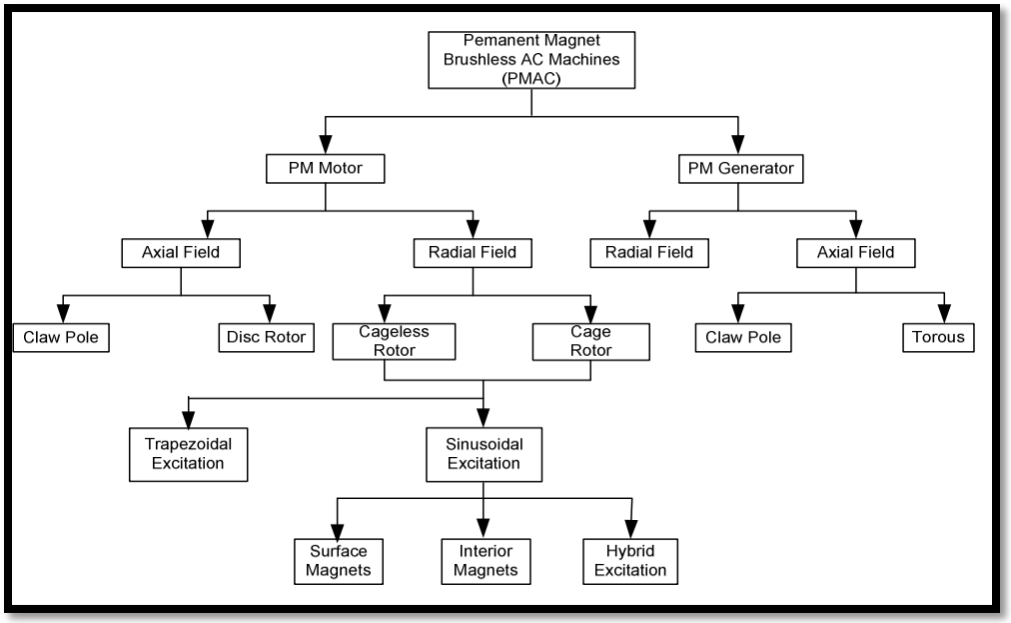

Figure 5. Classification of Permanent Magnet Magnate Machines [31].

The machine is classified as a generator and electric motor, with two types based on supply wave shape: PMBLDCM for square wave and SPMSM for sinusoidal wave.

3. Modeling of PMSM-Based WECS

The electric motor of PMSM can be modeled using mathematical equations, analyzing it from a three-phase system to a binary system using the theory of references [32].

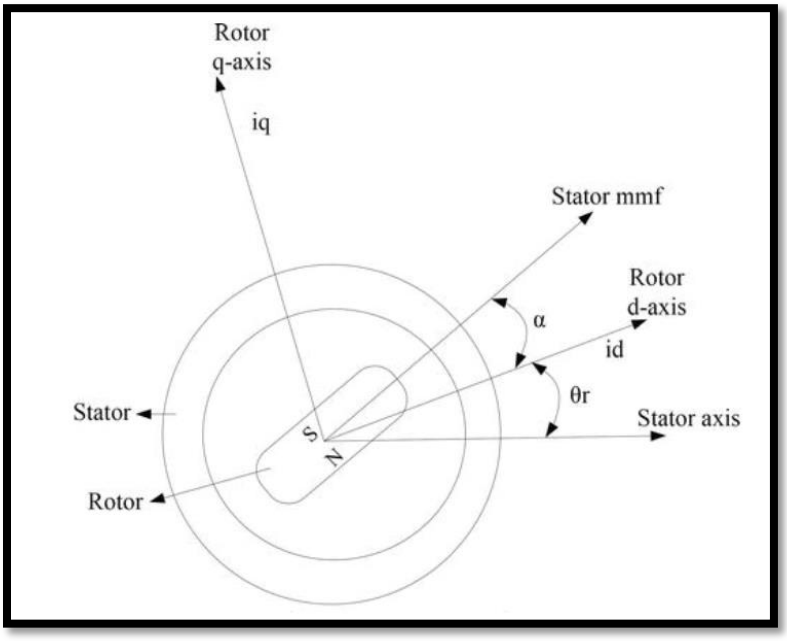

Figure 6. Axis motor [32].

The mathematical model of a permanent magnet synchronous generator is determined by the following statement in vector coordinates dq [32].

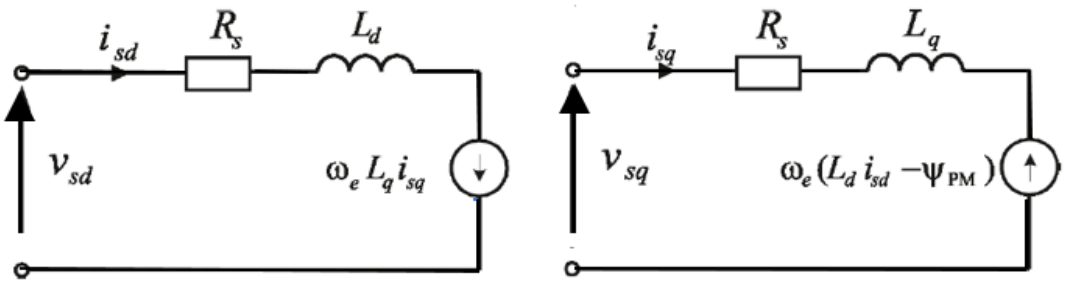

Figure. 7. The vector equivalent circuit (dq) of a permanent magnet synchronous generator [32].

$$\frac{d}{dt} i_d = \frac{1}{L_d} V_d - \frac{R}{L_d} i_d + p \cdot \omega_e \cdot i_d \quad (17)$$

$$\frac{d}{dt}i_q = \frac{1}{L_q}V_q - \frac{R}{L_q}i_d - p \cdot \omega_e \cdot i_d + \frac{\psi_r p\omega_e}{L_q} \quad (18)$$

The formulas and illustration suggest a sinusoidal shape for the element's EMF due to its amplitude and rotor location, figuring out a permanent magnet synchronous generator's electromagnetic torque [33, 34].

$$T_e = 1.5p\left[\psi_r i_q + \left(L_d - L_q\right)i_q i_d\right], \quad (19)$$

Where is the angular velocity of the rotor? The following values describe the amplitude of flux: vq is the q-axis voltage, vd is the d-axis voltage, iq is the q-axis current, id is the d-axis current, and R is the stator winding resistance.

where p is the number of pole pairs, r is the rotor's rotational velocity, iq, id, and vq are the q- and d-axis currents, Lq and Ld are the q- and d-axis inductance and voltage, respectively. Active power in the motor mode can be stated as follows as part of apparent power.

$$P_{em} = 1.5p\left[e_d i_d + e_q i_q\right] \quad (20)$$

$$e_d = -\omega_e L_q i_q = -\omega_e \psi_q \quad (21)$$

$$e_d = -\omega_e L_d i_d + \omega_e \psi_r = \omega_e \psi_q \quad (22)$$

Here, ed and eq stand for the flux connections of the dq-axes as well as the back EMFs in the vector coordinate system of the dq-axes. The active power may be expressed as follows:

$$P_{em} = 1.5\omega_e\left[\psi_d i_q - \psi_q i_d\right] \quad (23)$$

As a result, the electromagnetic torque generated by the PMSG is defined according to this [32, 33, and 34]:

$$T_e = \frac{P_{em}}{\omega_e / \frac{P}{2}} = \frac{3}{2}\left(\frac{p}{2}\right)\left[\psi_d i_q - \psi_q i_d\right]$$

$$T_e = 1.5p\left[\psi_r i_q + \left(L_d - L_q\right)i_q i_d\right] \quad (24)$$

4. Modelling of Power Electronic Part

The converter model consists of a frequency converter and starting block, with the inverter operating through a PWM switching pulse and a DC voltage link [34]:

$$V_a = L\frac{di_a}{dt} + Ri_a + V_{ra}$$

$$V_b = L\frac{di_b}{dt} + Ri_b + V_{rb}$$

$$V_c = L\frac{di_c}{dt} + Ri_c + V_{rc} \quad (25)$$

The voltage source's phase voltages are shown here by Va, Vb, and Vc. phase currents, Vdc is the DC output voltage, and C, DC bus smoothing capacitor on. ia, ib, and ic are the phase currents. A, B, and C in Vr. Following that, the source phase voltage is written as:

$$V_a = V_m \sin\theta$$
$$V_b = V_m \sin\left(\theta - \frac{2\pi}{3}\right)$$
$$V_b = V_m \sin\left(\theta - \frac{4\pi}{3}\right) \quad (26)$$

where V_m denotes the voltage value at its maximum. Is used to denote the input voltage of the inverter. Given that the work generates an alternating voltage using a bipolar switching paradigm, the value of Si (u, v, w) is (1, -1) if there is a two-state valve action. Following that, a matrix of three-phase functions with 6 times the switching time is used to represent the inverter voltage UN (u, v, w) [34]:

$$U_N \begin{bmatrix} a \\ b \\ c \end{bmatrix} = \frac{1}{3L_s} \begin{bmatrix} 2s_a & -s_b & s_c \\ -s_a & 2s_b & -s_c \\ -s_a & -s_b & 2s_c \end{bmatrix} \quad (27)$$

The matrices below [22] illustrate how this sequence might be characterized as follows:

Si (a, b, c) =

$[2s_a\ -s_b\ s_c\ -s_a\ 2s_b\ -s_c\ -s_a\ -s_b\ 2s_c]$ (28)

The following values must be designated for the dependency characterizing the inverter: R-coil resistance, L-inductance, Vdc-DC link voltage, and Si-state of the switching function for three states:

Si(i = a, b, c)

= {1 upper IGBT is ON 0 lower IGBT is ON

The conversion mode may be created [33]. Depending on the number of phases, Key Si changes. It adheres to the input voltage and current phase relationships.

This enables you to replicate the rectifier's behavior after processing the control algorithm's input parameters. The following (3.38) presents the standard mathematical relationship of arithmetic matrices [34].

$$\frac{d}{dt}\begin{bmatrix} i_a \\ i_b \\ i_c \end{bmatrix} = -\frac{R_s}{L_s}\begin{bmatrix} i_a \\ i_b \\ i_c \end{bmatrix} + \frac{1}{3L_s}\begin{bmatrix} 2s_a & -s_b & s_c \\ -s_a & 2s_b & -s_c \\ -s_a & -s_b & 2s_c \end{bmatrix} V_{dc} + \frac{1}{L_s}\begin{bmatrix} e_a \\ e_b \\ e_c \end{bmatrix}, \quad (29)$$

The excitation voltage UN may be found in matrices (3.37) linked to the machine-side parameters Rs and Ls as well as the inverter's three-phase alternating currents (ia, ib, and is). The rotating electromotive force (EMF), which the machine winding induces, is denoted in the formula as e (a, b, c)

5. Vector Control Method of PMSG

In a synchronous machine with permanent magnets, It is thought that the inductances along the d and q axes are equal, simplifying the torque equation.

$$T_e = 1.5p\left[\psi_r i_q\right] \quad (30)$$

The maximum torque is achieved by setting the d-axis current reference to zero, permitting the electromagnetic torque and q-axis current to have a linear relationship, allowing for vector control.

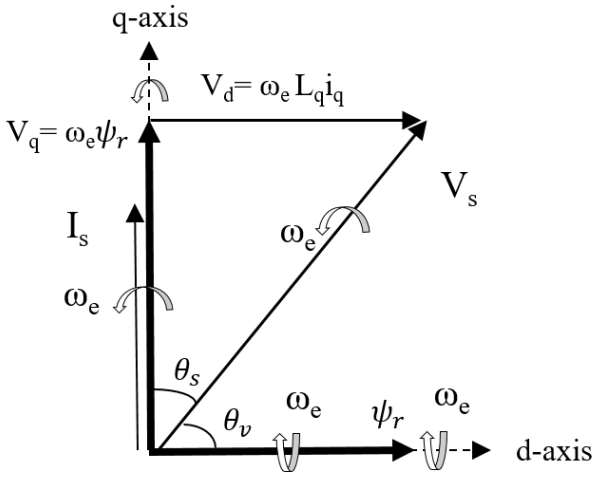

Figure 8. Shows a vector driven PMSG diagram [32].

To ensure vector control, the generator's spinning field value must be chosen, ensuring the axis and signal region align with the stator flux vector. In the process of converting a three-phase system (ABC) into a two-phase stationary coordinate system (α, β, system), the following formulas are used to adjust the phase count (Clark transform) [32]:

$$V_\alpha = V_A$$
$$V_\beta = \frac{V_B - V_c}{\sqrt{3}} \quad (31)$$

Equation 30 converts the number system's biaxial stationary values into rotational values via the Park transformation.

The Park transforms represent the. [32, 33, 34]:

$$V_d = V_\alpha \cos(\theta) + V_\beta \sin(\theta)$$
$$V_q = V_\beta \cos(\theta) - V_\alpha \sin(\theta) \quad (32)$$

The vector control approach for synchronous generators with permanent magnets is depicted in Figure 9, including wind speed, MPPT, wm, TSR, PI, SPWM, PMSG, and P number of poles.

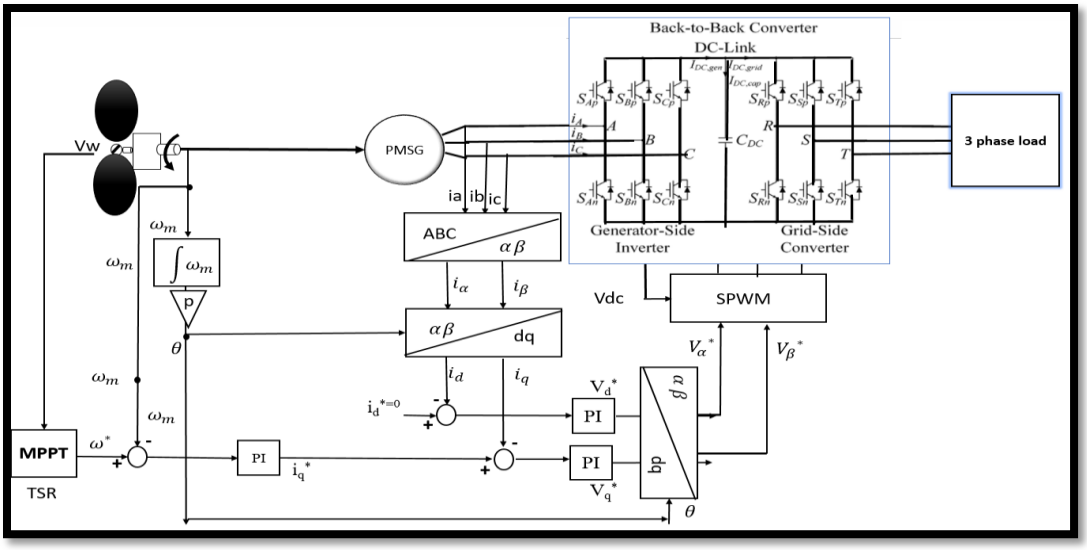

Figure 9. Vector control of PMSG – control strategies scheme

Based on the ideal propeller speed ratio, the generator power converter employs MPPT control in conjunction with a vector control strategy. The d-axis current control loop, q-axis current control loop, and speed control loop are the three feedback loops in the system. The generator's actual speed is contrasted with its reference value, and the PI controller manages the optimum speed value.

5. CONCEPTUAL FRAMEWORK

5.1 Factors Affecting Electricity Generation

Various obstacles in the form of buildings, trees, or neighboring wind turbines can reduce wind speeds.

Wind farms require precise placement and careful monitoring of individual turbine arrangements. In 2018, physicists discovered that arranging turbines unevenly can increase the average output of a single turbine by 30%, highlighting the importance of careful design [36–37]. Wind farm design should consider mutual turbine locations to reduce electricity production by up to 10%. Wind power issues can be addressed by increasing airflow and making it adjustable. Traditional methods involve increasing rotor working diameters or tower heights, but these methods can capture more wind energy and convert it into electricity [38]. As the rotor height increases, the average rotational speed also increases, with higher altitudes resulting in greater wind speeds, resulting in increased power production [39]. Engineers are primarily working on a method that increases rotors and mast heights, but this has limitations due to production and maintenance costs.

Small wind turbines face issues in power management, control elements, and on-off modes. A power regulation system for a PM generator uses two loops to stabilize wind power utilization and load power [40].

5.2 Development of wind energy conversion system

Chapter three presents a complete wind conversion system designed using mathematical analysis of mechanical wind turbines, electric generator, inverter, and load, utilizing a synchronous PMSG electric generator with SPWM control.

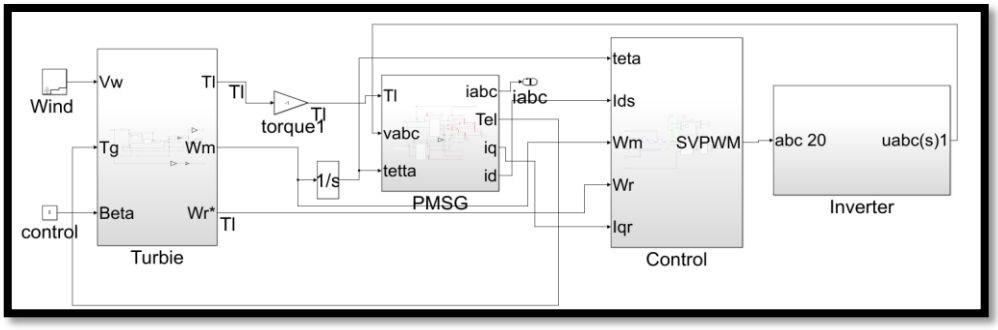

Figure 18. The model demonstrates an autonomous wind energy conversion system using a permanent magnet synchronous generator with vector control.

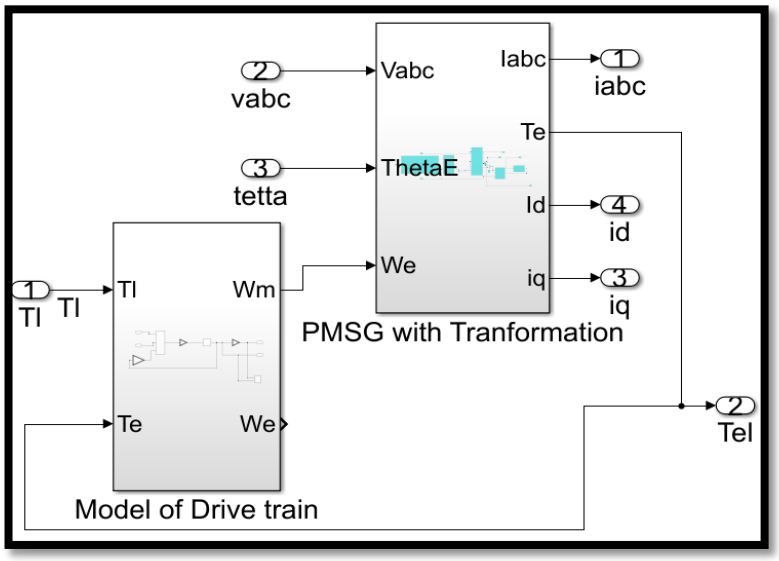

Figure 19. Direct drive of a permanent magnet synchronous generator.

The study analyzes a 6-kW wind turbine system in Iraq using MATLAB/Simulink, obtaining unique results for mechanical, electrical, and electronic systems using wind speed data.

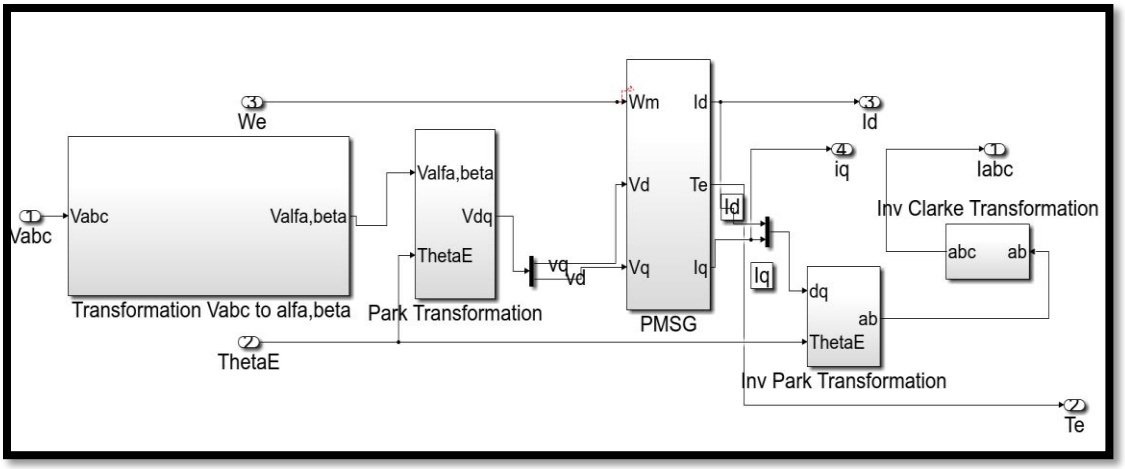

Figure 20. PMSG Blocks.

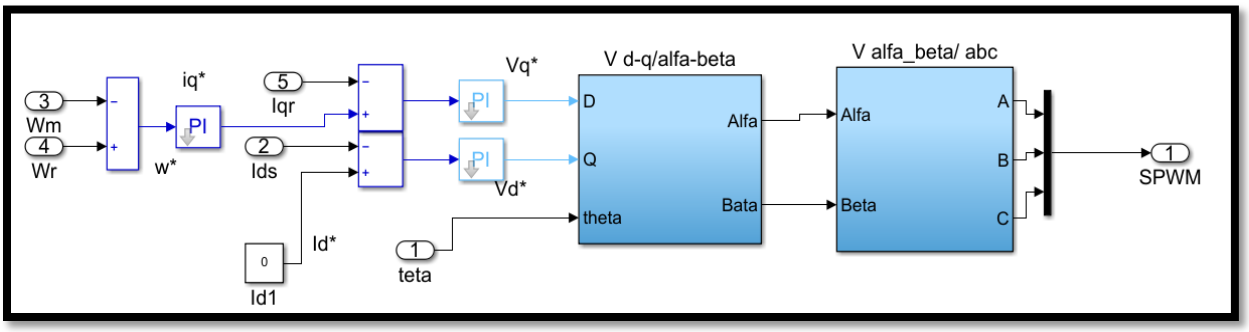

Figure 21. A vector control block based on the coordinate transformation scheme.

The parameters for authentic mechanical and electric generator models were sourced from renowned wind turbine and electric generator manufacturing firms, which were also utilized in studies and research. Figure 22 displays the power-speed relationship and turbine mechanical characteristics at a blade angle of attack $\beta = 0$ for various wind speed values (6-13 m/s). The study demonstrates the relationship between power and wind turbine speed and mechanical characteristics, illustrating the impact of blade angle and angular frequency on turbine rotation.

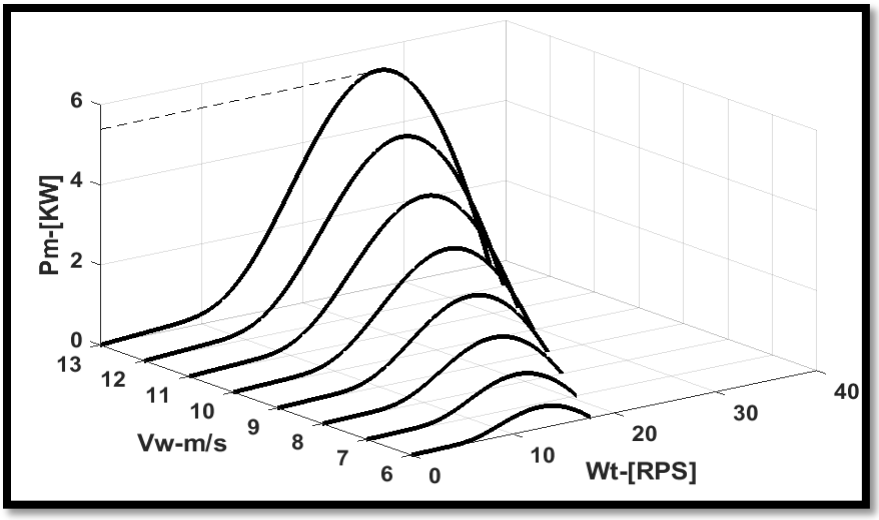

Figure 22. Dependence of turbine power on speed.

The maximum power maintenance mode (MPPT) controls the transition from one mechanical curve to another at maximum points for different wind speeds. The maximum power at the turbine output is 5.6 kW at a wind speed of 13 m/s. The characteristics of the PMSG and inverter frequency are calculated bellow

.

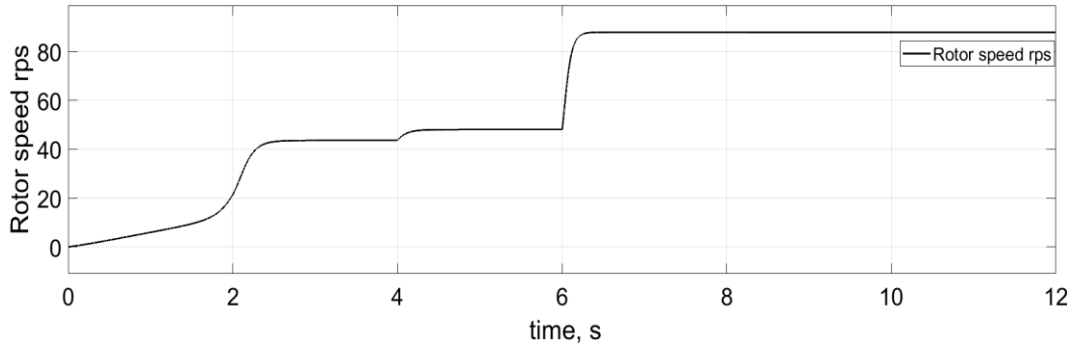

Figure 23. Rotor speed of generator with time.

Figure 23 shows the generator's speed changes with wind speed, reaching 800 revolutions per minute in 6 seconds.

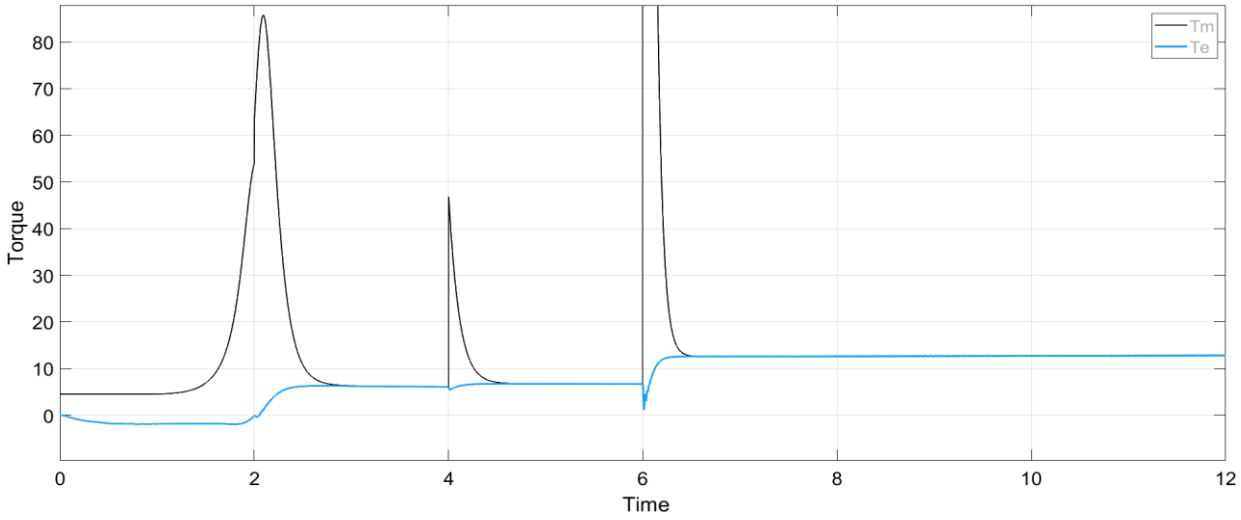

Figure 24. Electromagnetic torque of PMSG and mechanical torque from turbine

The development of the electromechanical system is successful when the torques of the electric generator and turbine increase with speed due to increased current. Current and voltage are generated by PMSG rotation.

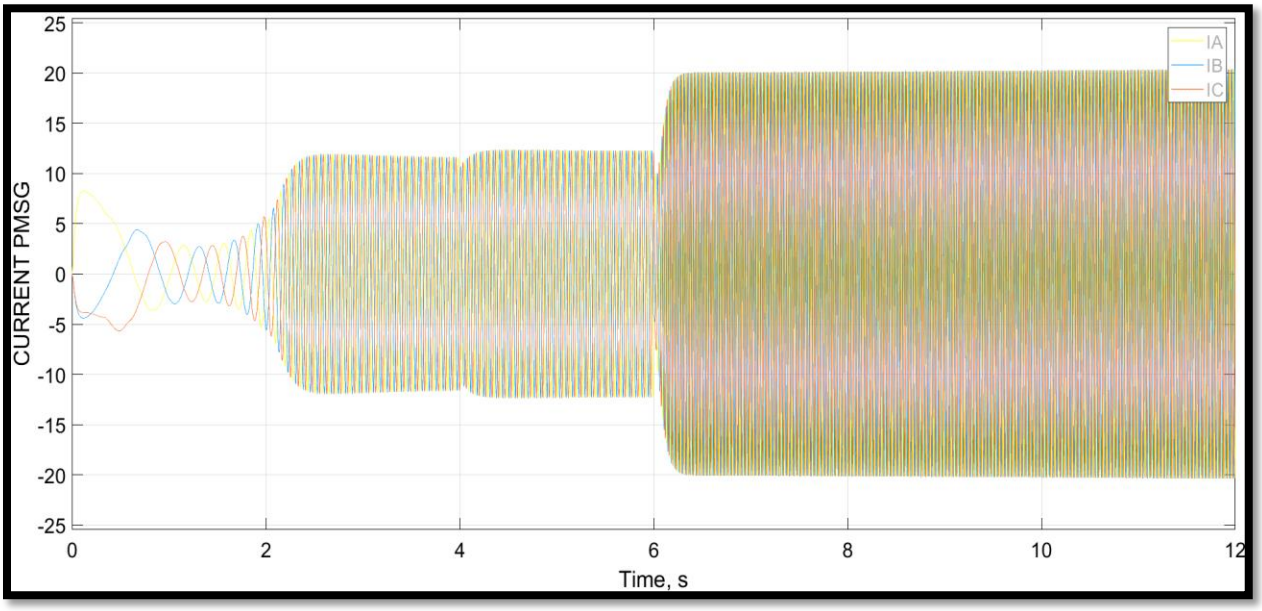

Figure 25. Three-phase current ABC from PMSG with time.

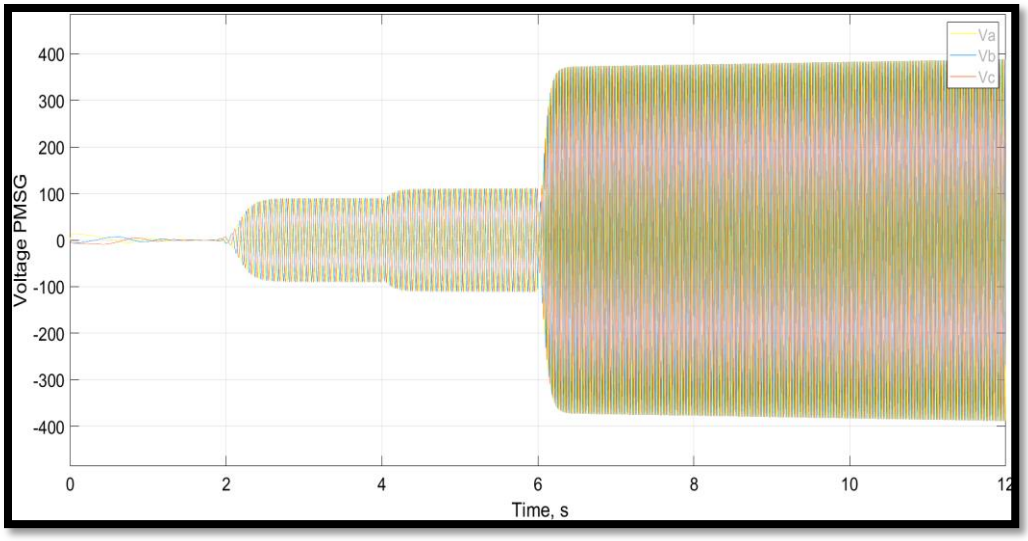

Figure 26. Three-phase voltage ABC from PMSG with time.

Figures above show that wind speed affects the three-phase current and voltage, resulting in increased control performance. High control reliability is observed as the current at 6 s equals 20 A and the voltage is 380 volts. The rated speed and current are also represented in 6 s. The PMSG permanent magnet synchronous generator's control system, using MPPT strategy, effectively extracts maximum wind turbine power and converts it into active electric power for consumer delivery, as demonstrated in simulation results.

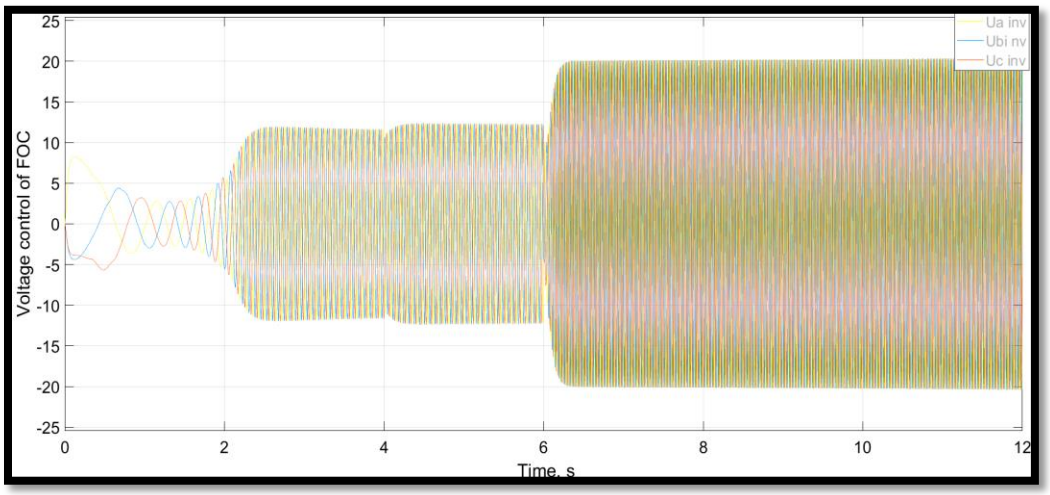

Figure 27. the signal control voltage from the FOC volte.

The required voltage for controlling inverter switches is not exceeding the required voltage, resulting in a theoretical control voltage of 20 volts. The efficiency of the

wind generator is dependent on the rotation speed of the PMSM rotor.

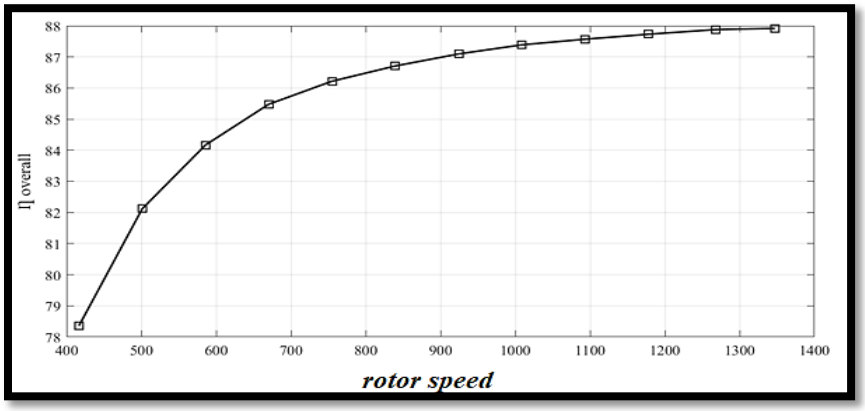

Figure 28. Dependence of efficiency on rotor speed. (RPM)

The wind generator's efficiency increases with wind speed, reaching 86.22% at a maximum speed of 8.8 m/s, indicating a continuous increase in input power.

6. Results and Discussion

Renewable energy, such as wind and solar, is gaining popularity due to its potential to provide electricity in isolated areas without causing greenhouse gas emissions or air pollution. This paper focuses on developing, implementing, and designing a wind energy model for Iraqi conditions, including wind turbines connected to an electric generator. The optimal locations and heights for generating energy in Iraq are identified, with the Basra site having the maximum potential. The electrical power product by the turbine was calculated for both cities to show which one is the best.

6.1 Calculation Studies for the Project Site at Nasiriyah

The average wind speeds during a year in Nasiriyah are shown in Fig 29.

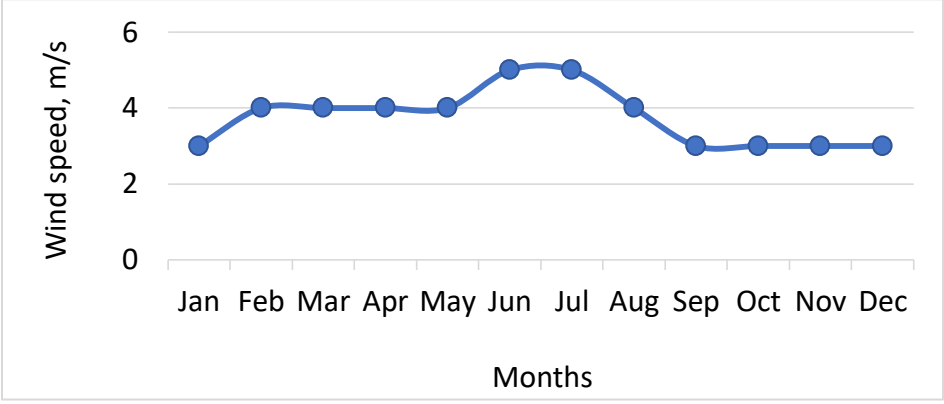

Figure 29. Average wind speed in Nasiriyah during the year.

Through year the wind speed started with 3 m/s and increase until reaches over 5 in July then decrease to 3. The instability in speed caused by the climate changing through seasons.

Next, wind speeds of a height of (20 and 50 m) at the hub level of the wind turbine hub were calculated by month (Fig 30).

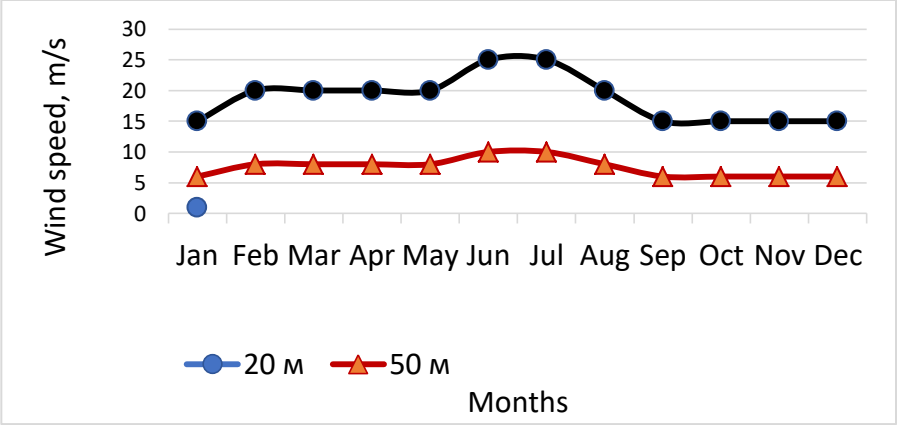

Figure 30. Average wind speed in Nasiriyah.

Nasa Power system data for 2020-2021 confirms an interval of average wind speed at 50 m altitude between 5-10 m/s. the values of speed increase with increasing of altitude, where high speed occur because the area is open and has no barriers to prevent air flowing.

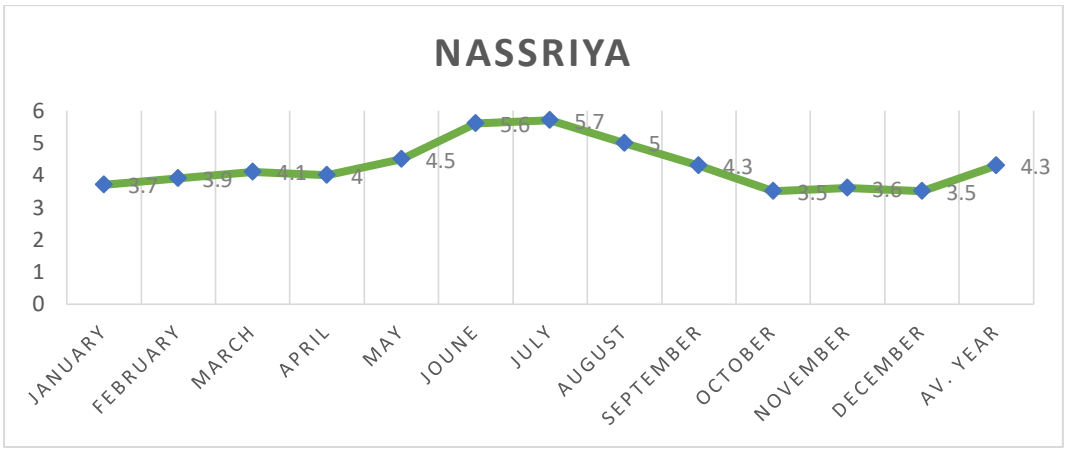

Figure 31. Wind speed in Nassriya city.

Recent studies reveal that Nassriya city experiences wind speeds ranging from 4 to 5.8 meters at an altitude of only 10 meters [42].

The Nasiriyah diagram shows those days in a month during which the wind speed reaches a certain value (Fig 32).

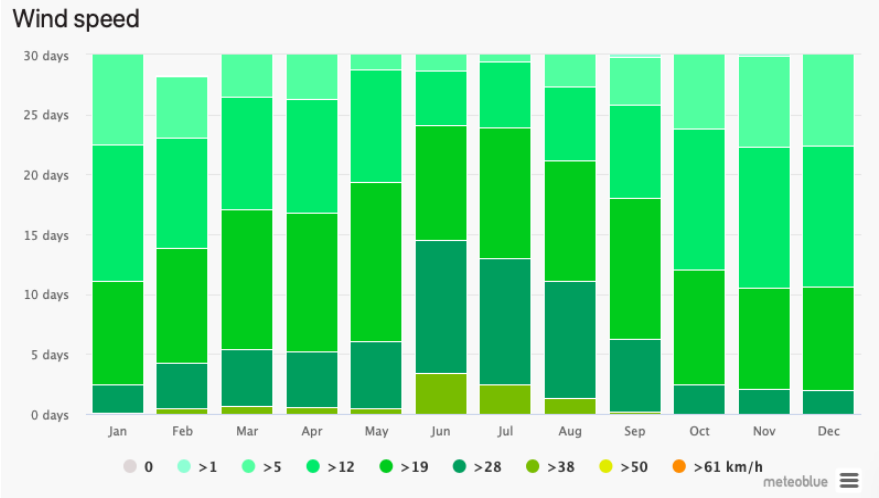

Figure 32. Wind speed changes in Nasiriyah.

the power generation of one freestanding wind turbine (height 20 + 50 m) without taking into account mutual shading by other wind turbines for one month (Kr = 98 %) [41]:

$$\text{Wone wpi} = 24 * 0{,}98 * \cdot (538{,}51 * 7 + 1051{,}25 * 5 + 1816{,}56 * 6 + 2884{,}63 * 5 + 6130{,}89 * 7) = 1817{,}29 \text{ kWh for 20m}$$

and

$$\text{Wone wpi} = 24 * 0{,}98 \cdot \cdot (538{,}51 * 5 + 1051{,}25 * 3 + 1816{,}56 * 7 + 2884{,}63 * 9 + 6130{,}89 * 6) = = 1912{,}39 \text{ kWh for 50m}$$

For one installation including auxiliary needs for one month:

1817*29·93 % = 1690,08 kWh

And

1912.39*93 % = 1778,53 kWh.

The projected annual output of marketable electrical energy of a wind turbine to the grid is determined according to the grid is approximately 20281 and 21342 kWh.

6.2

alculation Studies for the Project Site at Basra

The average wind speeds during a year in Basra are shown below.

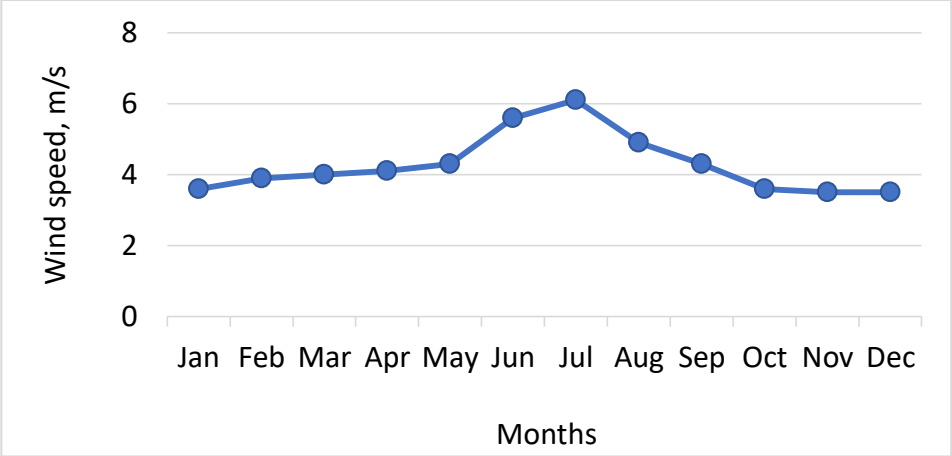

Figure 33. Average wind speed in Basra.

The Basra city indicate low wind speed through all months, where it started under 3 m/s and the max value reaches to approximate 6 m/s and then return to 3 because of its location at the south direction which influence deeply by comparing it with Nasiriyah.

Next, wind speeds at the hub level of the wind turbine hub were calculated by month.

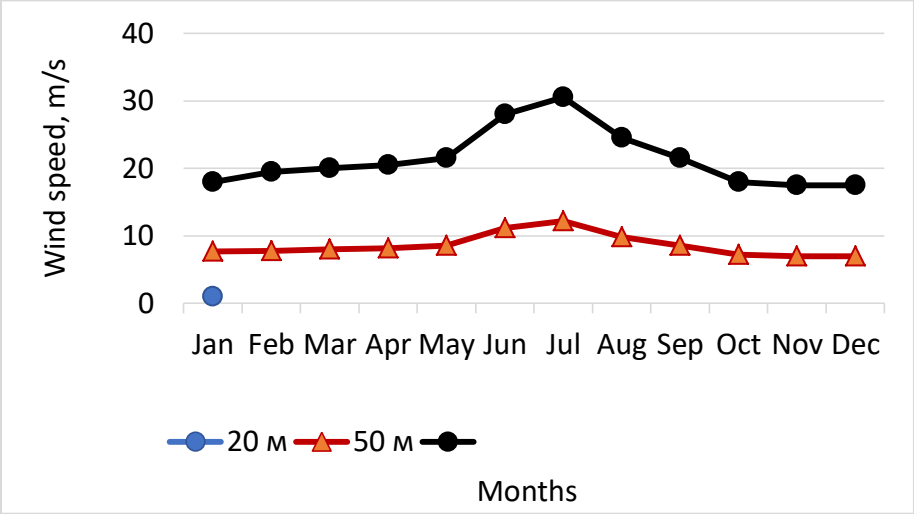

Figure 34. Average wind speed in Basra at a height of 20 m and 50 m.

NASA Power system data for 2020-2021 confirms an interval of average wind speed at 50 m altitude between 5-11 m/s. the altitude has same influence through all cities because in Iraq there are not vertical building with high level just horizontal constrictions.

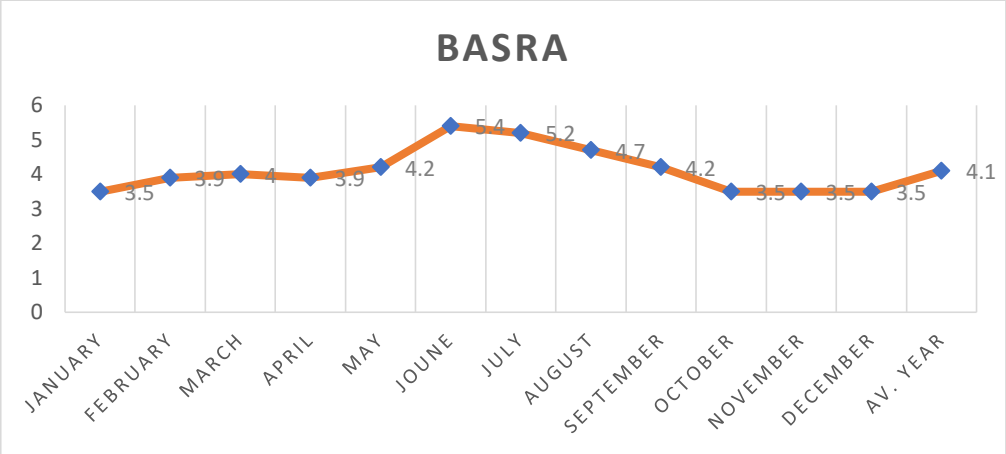

Figure 35. Wind speed in Basra city.

From the recently presented studies, we note that in the city of Basra, the wind speed ranges between 4 and 5.6 meters at an altitude of only 10 meters [42].

The Basra diagram shows wind speed days in a month, with monsoons producing strong winds from December to April and calm air currents from June to October.

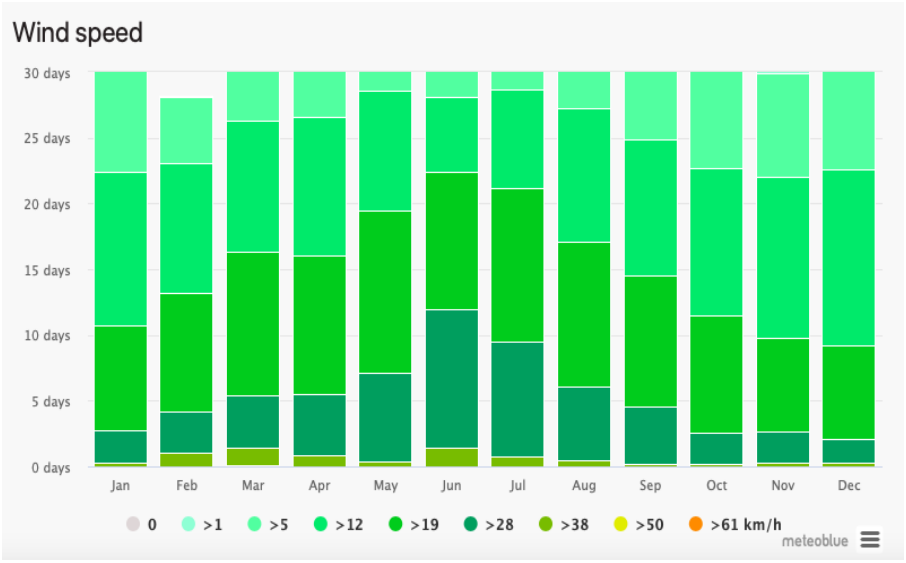

Figure 36. Diagram of wind speed changes in Basra.

For the given site, the power generation of one freestanding wind turbine (height 20 m) without taking into account mutual shading by other wind turbines for one month (Kr = 98 %) [41]:

$$\begin{aligned} \text{Wone wpi} = 24 * 0{,}98 * \\ * (1051{,}25 * 2 + 1816{,}56 * 4 \\ + 2884{,}63 * 4 + 4305{,}9 * 6 \\ + 6130{,}89 * 7 + 8410 * 7) \\ = 3493{,}4 \text{ kWh} \end{aligned}$$

For one installation including auxiliary needs for one month:

3493,4*93 % = 3248,86 kWh

The Basra site has the highest energy potential among all sites with the same wind turbine parameters, according to the grid's projected annual output of 38986 kWh.

7. Conclusions

The study developed an electromechanical system using MATLAB SIMULINK, including a turbine and a power generation-based permanent magnet machine. Two cities in Iraq (Nassriya and Basra) were taken to study the effect of wind speed throughout the year. The results indicate that in the first month of the year, the wind speed started with approximately equal values for both cities, while the difference appeared in the middle of the year, then returned to a decrease.

The highest wind speed is at Basra because of its location, where the maximum speed is above 6 m/s in July, but at AL-Nassriya, the speed reaches 5 m/s in the same month, and this difference is caused by the changing climate, where the weather in Basra has more humidity than in Nassriya. The altitude of the turbine has a deep effect on the work efficiency, where the high efficiency obtained at a high-level means that the wind turbine was built at a very high level to ensure that the wind speed was the highest, as indicated by the test. The 50 m latitude gives a higher speed than 20 m through all months of the year and for all cities because construction prevents it. At last, the usage of wind power in Iraq is increasing due to its excessive efficiency, highlighting the capacity of wind turbine converters with networks for renewable electricity. The system's general efficiency become 88.22%, indicating its durability and efficiency inside the Iraqi climate.

Conflict of Interest

The authors state no conflict-of-interest

Data availability statement

Most datasets generated and analyzed in this study are comprised in this submitted manuscript. The other datasets are available on reasonable request from the corresponding author with the attached information.

Statements and Declarations

Funding and/or Conflicts of interests/Competing interests. Also, I declare that the manuscript was done depending on the personal effort of the author, and there is no funding effort from any side or organization, as well as no conflict of interest with anyone

related to the subject of the manuscript or any competing interest.

REFERENCES

[1] Samokhvalov D.V., Jaber A.I., Filippov D.M., Kazak A.N., Hasan M.S. Research of Maximum Power Point Tracking Control for Wind Generator. IEEE Conference of Russian Young Researchers in Electrical and Electronic Engineering (EIConRus), 1301-1305(2020). doi: 10.1109/EIConRus49466.2020.9039180.

[2] M. A. Hannan 1,*ORCID,Ali Q. Al-Shetwi 2ORCID,M. S. Mollik 3,Pin Jern Ker 4ORCID,M. Mannan 1,M. Mansor 1ORCID,Hussein M. K. Al-Masri 5ORCID andT. M. Indra Mahlia 6ORCID. Wind Energy Conversions, Controls, and Applications: A Review for Sustainable Technologies and Directions. 22 February 2023, 15(5), 3986; https://doi.org/10.3390/su15053986.

[3] Jamal, A.; Suripto, S.; Syahputra, R. Multi-band power system stabilizer model for power flow optimization in order to improve power system stability. J. Theor. Appl. Inf. Technol. 2015, 81, 38202484.

[4] Hannan, M.; Lipu, M.H.; Ker, P.J.; Begum, R.; Agelidis, V.G.; Blaabjerg, F. Power electronics contribution to renewable energy conversion addressing emission reduction: Applications, issues, and recommendations. Appl. Energy 2019, 251, 113404.

[5] Oliveira, D.S.; Reis, M.M.; Silva, C.E.; Barreto, L.H.C.; Antunes, F.L.; Soares, B.L. A three-phase high-frequency semicontrolled rectifier for pm wecs. IEEE Trans. Power Electron. 2009, 25, 677–685.

[6] Ibrahim, R.A.; Zakzouk, N.E.J.A.S. A pmsg wind energy system featuring low-voltage ride-through via mode-shift control. Appl. Sci. 2022, 12, 964.

[7] Pande, J.; Nasikkar, P.; Kotecha, K.; Varadarajan, V. A review of maximum power point tracking algorithms for wind energy conversion systems. J. Mar. Sci. Eng. 2021, 9, 1187.

[8] Schreiber, A.; Marx, J.; Zapp, P. Comparative life cycle assessment of electricity generation by different wind turbine types. J. Clean. Prod. 2019, 233, 561–572.

[9] She, X.; Huang, A.Q.; Wang, F.; Burgos, R. Wind energy system with integrated functions of active power transfer, reactive power compensation, and voltage conversion. IEEE Trans. Ind. Electron. 2012, 60, 4512–4524.

[10] Mohammed H.J., Mohammed S.H., Faeza M. Study the Possibility of Application of Wind Turbine under the Climatic Conditions of Iraq. In Conference of Russian Young Researchers in Electrical and Electronic Engineering (ElConRus) (2022). 1234-1238.

[11] Al-Maamary H.M.S., Kazem H.A., Chaichan M.T. Changing the energy profile of the GCC States: A review. International Journal of Applied Engineering Research (IJAER), 11(3)(2016). 1980-1988.

[12] Al-Hussieni A. J. M. A prognosis of wind energy potential as a power generation source in Basra City, Iraq State. European Scientific Journal, 10(36)(2014). 163-176.

[13] What is Sustainable Energy and Why Do We Need It? Retrieved from https://www.routledge.com/blog/article/what-is-sustainable-energy-and-why-do-we-need it#:~:text=Sustainable%20energy%20includes%20any%20energy,answer%20to%20our%20energy%20needs at 2023, May 21.

[14] Al-Kharbosy M. E. H. Enhancement protection and operation of the doubly fed induction generator during grid fault. South Valley University. (2012). Qena, Egypt.

[15] What is Horizontal Axis Wind Turbine: Working & Its Applications. Retrieved from https://www.elprocus.com/horizontal-axis-wind-turbine/ at 2023, May 21.

[16] Martinello, D., Emerson , G.C., Jean, P. da Costa, Cardoso R., Stein M.O.C. Emulation of wind turbines. Wind Turbines. Design, Control and Applications. (2016). doi: 10.5772/63448

[17] Samokhvalov, D.V., Jaber A.I. Estimation of the Maximum Efficiency and Mechanical Performance Output from Wind Turbine. XXII International Conference on Soft Computing and Measurements (SCM). 81-84(2019). doi: 10.1109/SCM.2019.8903847.

[18] Iraq-A Comparative Study. In IOP Conference Series: Materials Science and Engineering, 928(2)(2020). 022044.

[19] Norouztabar R., Mousavi A. S.S., Mousavi S.S., Nejat P., Rahimian K., S.S., Eldessouki, M. On the Performance of a Modified Triple Stack Blade Savonius Wind Turbine as a Function of Geometrical Parameters. Sustainability, 14(16)(2022). 9816. doi.org/10.3390/su14169816.

[20] Overview of Iraq's Renewable Energy Progress in 2019. Retrieved from https://iraqenergy.org/2020/02/20/overview-of-iraqs-renewable-energy-progress-in-2019/ at 2023, May 28.

[21] Boles M., Cengel Y. An Engineering Approach. New York: McGraw-Hill Education (2014).

[22] Bashaer M., Oday I. A., A. I. Al-Tmimi. Investigation and analysis of wind turbines optimal locations and performance in Iraq. FME Transactions, 48(1)(2020). 155-163.

[23] Ministry of Agriculture, unpublished data.

[24] Alhmoud L, Al-Zoubi H. IoT Applications in Wind Energy Conversion Systems. Open Engineering. 2019;9(1): 490-499. https://doi.org/10.1515/eng-2019-0061.

[25] Michael E, Tjahjana D, Prabowo A. Estimating the potential of wind energy resources using Weibull parameters: A case study of the coastline region of Dar es Salaam, Tanzania. Open Engineering. 2021;11(1): 1093-1104. https://doi.org/10.1515/eng-2021-0108.

[26] Al-Taai O. T., Qassim M. W., A. I. Al-Tmimi. Assessment of a viability of wind power in Iraq. American Journal of Electrical Power and Energy Systems. (2014). 3(3), 60-70.

[27] Panofsky H, Dutton J. Atmospheric Turbulence: models and methods for engineering applications. (1984). Pennsylvania State University: John Wiley and Sons.

[28] Samokhvalov D. V, Jaber A. I. Estimation of the Maximum Efficiency and Mechanical Performance Output from Wind Turbine. XXII International Conference on Soft Computing and Measurements (SCM). 81-84(2019). doi: 10.1109/SCM.2019.8903847.

[29] Ahmed S.T. A review of solar energy and alternative energies applications in Iraq. The First Conference between Iraqi and German Universities DAAD, (2010) Arbil, Iraq.

[30] Balashanmugham A, Mockaisamy M. Permanent-magnet synchronous machine drives. In Applied Electromechanical Devices and Machines for Electric Mobility Solutions. Intech Open.

[31] Dwivedi, S.K., Laursen, M., Hansen, S. Voltage vector based control for PMSM in industry applications. IEEE International Symposium on Industrial Electronics. Bari, Italy, 3845-3850(2010). doi: 10.1109/ISIE.2010.5637742.

[32] Jaber A. I. J. Autonomous wind energy converter based on BLDC machine. Topic of the dissertation on the Higher Attestation Commission of the Russian Federation 05.09.03(2022). Candidate of Sciences, Russia-Sainte Petersburg.

[33] Jaber A.I., Samokhvalov D.V., Al-Mahturi F.S., Filippov D.M., Kazak A.N. Power Losses Calculation in Wind Power Plant based on a Vector-Controlled Permanent Magnet Synchronous Generator. IEEE Conference of Russian Young Researchers in Electrical and Electronic Engineering (ElConRus), 917-921(2021). doi: 10.1109/ElConRus51938.2021.9396514.

[34] Samokhvalov D.V., Jaber A.I., Almahturi F.Sh. Maximum power point tracking of a wind-energy conversion system by vector control of a permanent magnet synchronous generator. Russian Electrical Engineering, 92(3)(2021). 163-168.

[35] Induction Generator Working Principle, Induction Generator Types, Retrieved from https://electengmaterials.com/induction-generator-working-principle/ at 2023, May 20.

[36] Lee M., Nathaniel A B., David W K., Axel K. Two methods for estimating limits to large-scale wind power generation. Proceedings of the National Academy of Sciences, 112(36)(2015). doi: 10.1073/pnas.1408251112.

[37] GE Renewable Energy. Retrieved from https://www.ge.com/renewableenergy/ wind-energy/ turbines at 2023, June 11

[38] Jang K.-H., Ryu K.-W. Blade Design and Aerodynamic Performance Analysis of a 20 MW Wind Turbine for LCoE Reduction. Energies, 16, 5169(2023). doi.org/10.3390/en16135169.

[39] Wind Turbines: the Bigger, the Better. Office of Energy Efficiency & Renewable Energy, 2022. Retrieved from https://www.energy.gov/eere/articles/wind-turbines-bigger-better at 2023, June 11.

[40] Dzhaber, A.I., Al Makhturi, F.Sh., Samokhvalov, D.V. Power losses in a wind turbine in the mode of maintaining maximum power at vector control of a synchronous generator. LETI Transactions on Electrical Engineering & Computer Science, 2(2021). 77-82.

[41] Al-Hussieni A. J. M. A prognosis of wind energy potential as a power generation source in Basra City, Iraq State. European Scientific Journal, 10(36)(2014). 163-176.

[42] H. J. Mohammed, M. S. Hasan, F. Mahdihadi, K. Nikolay V. Study the Possibility of Application of Wind Turbine under the Climatic Conditions of Iraq, Conference of Russian Young Researchers in Electrical and Electronic Engineering (ElConRus), Saint Petersburg, Russian Federation, 2022, pp. 1234-1238, doi: 10.1109/ElConRus54750.2022.9755597.